Damping capacity, resistivity, thermal expansion and machinability of aluminium alloy-mica composites

DEONATH
Institute of Technology, Banaras Hindu University, Varanasi 221 005, India

RAM NARAYAN, PRADEEP K. ROHATGI*
Regional Research Laboratory, Council of Scientific and Industrial Research, Trivandrum 695 019, India

Damping capacities of cast aluminium alloy—mica particle composites were measured using a torsional pendulum method at a constant strain amplitude. The damping capacity of aluminium alloys progressively increases with increasing amounts of mica particles dispersed in the matrix, within the range investigated. The percentage increase in damping capacity at any level of mica is several times greater than the volume per cent of mica particles present in the matrix. The ratios of the specific damping capacity to density of aluminium alloy—mica particle composites (above 2% of mica) are greater than that of cast iron. Machinability tests on aluminium alloy—mica composites carried out at different speeds indicated that the average length and weight of individual chips decreases with increasing amounts of mica particles in the matrix. The percentage increase in the number of chips per gram of composite was several times the volume per cent of mica particles present in the composite. A decrease in the size of chips due to mica dispersions is a major asset since it permits faster machining speeds. Measurements of coefficient of thermal expansion showed very marginal increases in the aluminium alloys as a result of 2% mica dispersions. The electrical resistivity measurements of aluminium—mica composites using Kelvin's double bridge showed increases in electrical resistance of the order of 14% as a result of 2.2% mica additions. The measured increases in the electrical resistivity and coefficients of expansion are higher than the values calculated from the presently established theories of composite materials.

1. Introduction

Metal—ceramic particulate composites consist of dispersions of ceramic particles in metal matrixes and they find application as electrical contacts, cutting tools, rocket nozzels, spark-plug electrodes, bearings and pistons. The conventional method of making such composites is generally powder metallurgy wherein the metal and ceramic powders are mixed, pressed and sintered. However, a relatively simple method of making cast particulate composites has been developed during the last decade which involves mixing of ceramic particles in a vortex created by mechanical stirring of liquid alloys and casting the melt containing suspended particles into permanent moulds [1—15]. Aluminium alloy—mica composites made by the above techniques have been shown to possess good anti-friction properties under boundary lubrication and under semi-dry conditions [16]. However, a good material for bearing applications should also have a

*Present address: Regional Research Laboratory (Bhopal), Council of Scientific and Industrial Research, 1 Rafi Marg, New Delhi 110001, India.

TABLE I Chemical analysis of cut mica powder

Constituents	Percentage (wt)
SiO_2	48.12
Loss on ignition	4.78
Fe_2O_3	3.10
Al_2O_3	33.06
CuO	1.62
MgO	1.13
K_2O	7.10
Na_2O	0.75
Li_2O	0.33

high damping capacity and good machinability. In this investigation the damping capacity and length of chips (one of the criteria for good machinability) of aluminium—mica composites with increasing mica contents in the matrix have been measured. Aluminium—mica particle composites, due to their antifriction properties, may also be useful as electrical contacts; therefore, in the present work the electrical resistance and coefficient of expansion of aluminium—mica composites were also measured.

2. Experimental procedure

Al—4 wt % Cu alloy was melted in a super salamander crucible using an oil-fired furnace and was superheated to 800° C. The melt was de-gassed with nitrogen. It was then stirred with a mechanical stirrer to obtain a vortex in the melt. Cut mica powder of average size 40 μm, prepared by milling muscovite mica sheets of the composition given in Table I, along with magnesium pieces (0.5×10^{-2} m to 1.0×10^{-2} m cubes), were added to the surface of the melt forming a vortex; the molten alloy containing suspended mica particles was de-gassed with a stream of nitrogen while stirring it slowly. The stirrer was removed and the

metal was poured into permanent moulds to obtain castings of the composites. A detailed description of the process is given elsewhere [15]. Since the density of mica particles is close to that of the matrix, the volume percentages of mica were almost the same as their weight percentages.

Damping capacity test pieces were machined from 2.5×10^{-2} m diameter cast rods, while 6.2×10^{-2} m diameter cylindrical castings were made for machinability test specimens.

2.1. Damping capacity tests

The damping capacity of aluminium alloy—mica composites was measured using a torsion pendulum method similar to that used by Rohatgi et al. [17] for measuring the damping capacity of aluminium—graphite composites. The dimensions of the sample and the apparatus used are shown in Fig. 1. A cast iron sample was also tested to compare the values obtained with the present set-up with the standard values reported in the literature, as a check on the experimental procedures. The tests were carried out at a shear stress level of 1.41×10^6 kg m^{-2} for aluminium alloys and at 2.10×10^6 kg m^{-2} for cast iron [18—20].

2.2. Measurement of electrical resistivity

Electrical resistance of mica dispersed aluminium alloy was measured using Kelvin's double bridge to eliminate the errors due to contact and lead resistance and to carry out precise measurements of low resistances. The size of the samples used was 2×10^{-2} m in diameter and 20×10^{-2} m to 30×10^{-2} m in length.

2.3. Measurement of coefficient of thermal expansion

A "Leitz" photographic dilatometer was used to

(a)
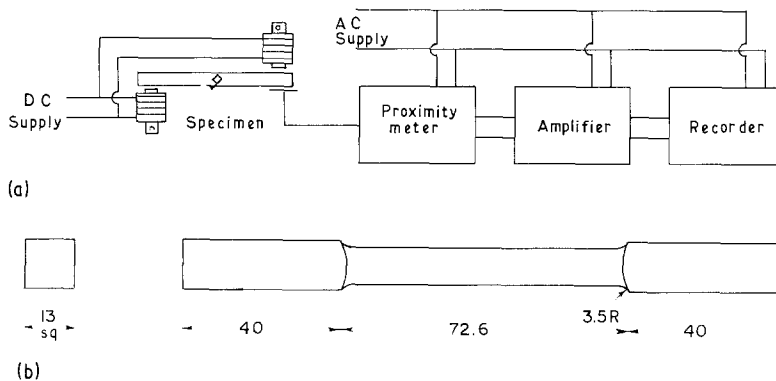
(b)

13 sq   40   72.6   3.5 R   40

Figure 1 Schematic diagram of (a) the apparatus and (b) the specimen (mm) used for damping capacity test. The necking diameter is 9 mm.

Figure 2 Macrophotograph of a typical bearing casting of Al−4.0 wt % Cu−1.5 wt % Mg 1.5 wt % mica composite.

measure the coefficient of thermal expansion. Samples, 3×10^{-3} m in diameter and 50×10^{-3} m long, were made from pure aluminium, Al−4 wt % Mg and Al−4 wt % Cu−1.1.5 wt % Mg−mica alloys. The samples were put in a quartz tube which was symmetrically arranged in a tube furnace. The temperature of the furnance was raised until the temperature of the samples recorded by the thermocouple reached 500° C. The expansion of the sample was recorded by a light spot moving on a photographic plate. Each point on the curve obtained by this method has for its ordinate the difference of dilations of the specimen and the standard; the abscissa is proportional to the dilation of the standard with respect to the quartz tubes.
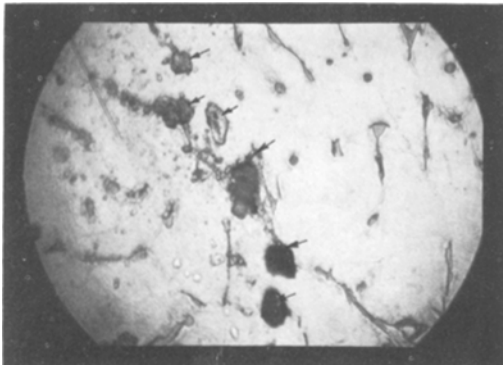

Figure 4 Scanning electron microphotograph of the fractured surface of cut mica dispersed Al−4.0 wt % Cu−1.5 wt % Mg−1.7 wt % mica composite (arrows indicate mica particles) (× 80).

2.4 Machinability test

The machinability tests were carried out by machining 5.5×10^{-2} m diameter and 15×10^{-2} m long specimens using 3×10^{-3} m and 1.5×10^{-3} m depths of cut. The top rake and side rake angles were kept at 20° each while the front and side clearances were fixed at 10° each, the nose radius of the tool was 0.50×10^{-3} m. The side cutting angle was 10° and the end cutting edge angle was 5°. The feed rate used was 1.1378 m sec^{-1}. When the depths of cut were 3×10^{-3} m and 1.5×10^{-3} m, the spindle speeds were 220 and 646 rpm respectively. The number of chips produced per gram of the material removed were counted.

Figure 3 Microstructure of Al−4.0 wt % Cu−1.5 wt % Mg−3.0 wt % mica (arrows indicate mica particles) (× 210).
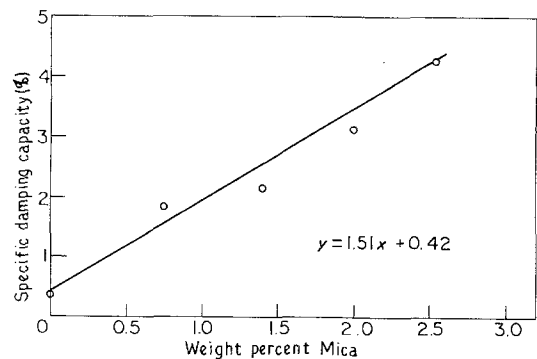

Figure 5 Specific damping capacity of mica dispersed Al−4.0 wt % Cu−1.5 wt % Mg alloy as a function of weight per cent mica.
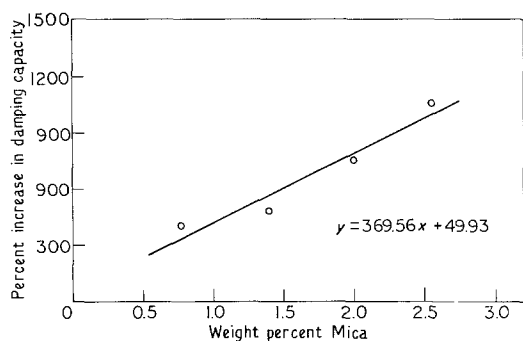
Figure 6 Percentage increase in damping capacity of mica dispersed Al−4.0 wt % Cu−1.5 wt % Mg alloy as a function of weight per cent mica.

3. Results and discussion

3.1. Damping capacity

A typical macrostructure, microstructure and fractograph of Al−4 wt % Cu−1.5 wt % Mg−mica particle composite alloy are shown in Figs 2, 3 and 4, respectively. The specific damping capacity of composites increases with mica percentage (Figs 5 and 6). The log decrement and specific damping capacity (SDC) to density ratio of several aluminium alloy−mica composites (Table II) show increasing damping capacity of the composites with percentage of mica. The ratio of SDC to density of some aluminium−mica particle composite exceeds that of cast iron above the 2% mica level.

Fig. 4 shows a tensile fracture surface with some voids around the particles, suggesting a relatively weak particle−matrix bond. Therefore in the aluminium−mica composite there is more likelihood of energy dissipation at the matrix−particle interface (by microplastic deformation or void formation) than within the mica particle.

The per cent increases (Table III) in damping capacity with a given volume per cent of 40 μm-sized flake-shaped mica dispersions are lower than the increases in damping capacity with the same volume percentages of 350 to 550 μm-sized spheroidal graphite dispersions (even though the matrix−particle interfacial area is much greater in the former). Apparently the nature of the particles is a more important factor than the interfacial area or the nature of the interface in influencing the damping capacity. Graphite particles may be more effective than mica in increasing the damping capacity since their shear strength is twenty times lower [21] than mica and can dissipate considerable energy in microplastic deformation of the particle itself.

3.2 Machinability

The number of chips produced per gram when machining the composites under specified conditions increases with increasing amounts of mica in the composites (Table IV, Fig. 7).

Fig. 8 shows a scanning photograph of a typical machined surface indicating that some mica particles are retained in the matrix during machining. These mica particles apparently introduce discontinuities in the material and act as stress raisers, thereby resulting in the frequent fracture of chips during machining. The production of small chips is one of the criteria of good machinability, since very long chips have a tendency to wrap around the tool at high machining speeds, limiting the rate of machining; the aluminium industry [22] is constantly in need of fast machining alloys.

3.3. Coefficient of thermal expansion

Additions of mica lead to a very slight increases in the coefficient of expansion of the alloys (Table V). The measured values of the coefficients of expansion are slightly lower than the values calculated according to either the rule of mixtures

TABLE II Damping capacity of mica dispersed aluminium alloy

Composition (wt %)	Log decrement	SDC (%)	SDC to density ratio
Al−4 Cu−1.5 mica	0.00206	0.37	0.13
Al−4 Cu−1.5 Mg−0.75 mica	0.0096	1.83	0.60
Al−4 Cu−1.5 Mg−1.0 mica	0.0112	2.14	0.79
Al−4 Cu−1.5 Mg−2 mica	0.0170	3.12	1.15
Al−4 Cu−1.5 Mg−2.55 mica	0.0220	4.24	1.57
Grey cast iron (quasi flake graphite)	0.0346	7.5	1.04
(See Fig. 3 of [19]) C = 3.4%, Si = 2.0%,			
Mn = 6.10%, S = 0.015%, P = 0.013%, Ni = 0.13%,			
Mg = 1.2%			

TABLE III Percentage increase in damping capacities of aluminium alloy—mica particle composites and aluminium alloy—graphite particle composites as a result of dispersed particles

Reference	Particle (wt %)*	Particle size (μm)	Percentage increases in specific damping capacity due to dispersed particles
Rohatgi et al. [17]	0.92 graphite	302	1390
	1.226 graphite	302	1392
	2.05 graphite	546	1950
	3.42 graphite	546	2110
Present investigation	0.75 mica	40	394.6
	1.40 mica	40	478.3
	2.00 mica	40	743.24
	2.55 mica	40	1045.90

*The weight and volume percentages are almost same for mica, the volume percentages of graphite will be slightly higher than their weight percentages.

[23] or the Thomas formula [24]; of the two formulas, the rule of mixtures gives values closer to the measured values.

The slight discrepancy between the measured and calculated values of the coefficient of thermal expansion could be due to (a) the anisotropic nature of mica with different coefficients of expansion in different crystallographic directions, (b) the lack of perfect bonding between the metal matrix and the mica particles and (c) the flaky shape of the mica particles requiring modifications in the expressions developed for either fibres or spherical dispersions.
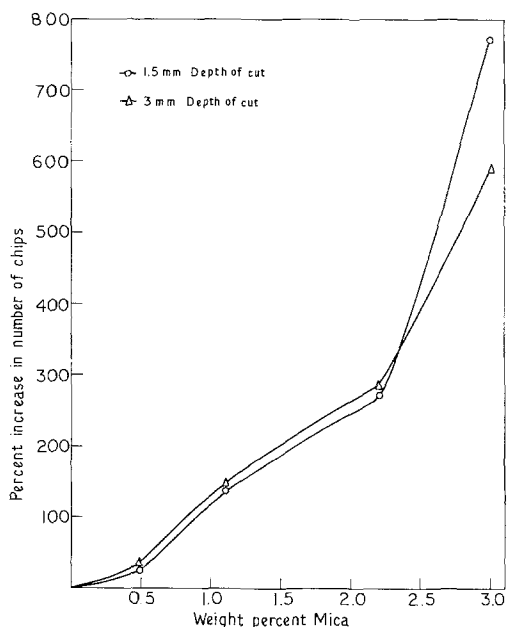
Figure 7 Percentage increase in number of chips per gram of mica dispersed in Al—4.0 wt % Cu—1.5 wt % Mg alloy as a function of weight per cent mica.

3.4. Electrical resistivity

The electrical resistivity of composite alloys increases with mica content (Figs 9 and 10). The percentage increases in the resistivity due to mica additions are many times the percentage of mica added. Since mica has a very high electrical resistance [25], of the order of 10^{19} to 10^{23} $\mu\Omega$m for muscovite compared to the matrix aluminium alloy of 3.6×10^{-6} $\mu\Omega$m, an increase in electrical resistance due to mica additions is expected. However, the observed increases in resistivity are more than the increases estimated according to the following three formulae available in the literature for resistance of particulate composites (Table VI).

The Maxwell formula [26, 27] for the specific resistance of a system where one phase is dispersed within another is

Figure 8 Scanning electron microphotograph of a typical machined surface of Al—4 wt % Cu—1.5 wt % Mg—2.0 wt % mica composite ($\times$ 72).

Figure 9 Resistivity of Al−4.0 wt % Cu−1.5 wt % Mg alloy as a function of weight per cent mica.

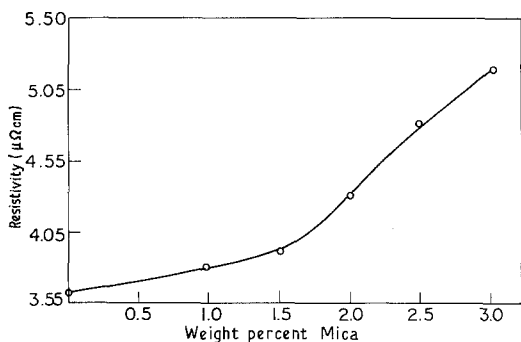*Figure 10* Percentage increase in the resistivity of Al− 4.0 wt % Cu−1.5 wt % Mg alloy as a function of weight per cent mica.

$$\rho = \left[\frac{2\rho_d + \rho_m + V_d(\rho_d - \rho_m)}{2\rho_d + \rho_m - 2V_d(\rho_d - \rho_m)} \right] \rho_m, \quad (1)$$

where ρ_m is the electrical resistivity of the matrix, ρ_d is the electrical resistivity of dispersoids, V_m is the volume fraction of the matrix and V_d is the volume fraction of the dispersoids.

When the resistance of the dispersoids is very high compared to the matrix, namely $\rho_d \gg \rho_m$, as in the case of mica dispersions in aluminium, this equation simplifies to

$$\rho = \left(\frac{2 + V_d}{2 - 2V_d} \right) \rho_m. \quad (2)$$

According to Van Beek [28] the electrical resistivity of a system containing spherical inclusions of an insulating material in a highly conducting material is given by

$$\rho = \frac{\rho_m}{1 - 1.5 V_d}. \quad (3)$$

The resistance of two phases [27] in parallel is given by

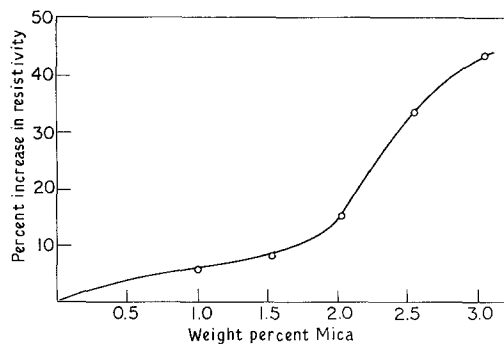$$\rho = \frac{\rho_m \rho_d}{V_m \rho_d + V_d \rho_m}. \quad (4)$$

This equation has been investigated since mica is in the form of flakes and these would be analogous to microscopic regions of parallel configuration in some locations. Table VI shows that, while values calculated according to all three formulae are higher than the measured values, the closest agreement is with Equation 3 derived by Van Beek [28]. The differences between the measured values and calculated values of electrical resistivity may be due to the following reasons:

(a) Lack of perfect bonding between the mica particles and the matrix;

(b) The presence of porosity in the cast composites which can lead to an increase in electrical resistance;

(c) The mica particles are flake-shaped and the formulae derived for spherical particles require modification;

(d) Some of the particles may be present as agglomerates;

(e) Mica is anisotropic and the electrical resistivity values will vary depending upon particle orientation (this has not been taken into account).

Table VI shows that additions of 2% mica (levels at which the composites can run even under dry

TABLE IV Results of machinability tests on mica dispersed aluminium alloys at a feed rate of 1.1378 m sec^{-1}

Sample number	Mica (%)	Depth of cut ($\times 10^{-3}$ m)	rpm	Number of chips per 10^{-3} kg
1	0	1.5	646	80
2	0.5	1.5	646	100
3	1.1	1.5	646	190
4	2.2	1.5	646	300
5	3.0	1.5	646	700
6	0	3.0	220	65
7	0.5	3.0	220	85
8	1.1	3.0	220	156
9	2.2	3.0	220	250
10	3.0	3.0	220	452

3030

TABLE V Measured and calculated values of coefficients of thermal expansion of cast Al–4 wt % Cu–1.5 wt % Mg–mica particle composites

Alloy composition (wt %)	Volume fraction of matrix, V_m	Volume fraction of dispersed mica, V_d	Coefficient of expansion ($^\circ C^{-1}$) (theoretically calculated values)[*]		
			Measured value	Rule of mixtures $\alpha = \alpha_m V_m + \alpha_d V_d$	Thomas formula $\alpha = (\alpha_m)^{V_m} \cdot (\alpha_d)^{V_d}$
Al–4 Cu–1.5 Mg	1.00	0.00	23.5×10^{-6}	23.5×10^{-6}	23.5×10^{-6}
Al–4 Cu–1.5 Mg–1.2 mica	0.988	0.012	23.8×10^{-6}	23.65×10^{-6}	23.62×10^{-6}
Al–4 Cu–1.5 Mg–2.2 mica	0.978	0.022	24.0×10^{-6}	23.78×10^{-6}	23.72×10^{-6}

[*]Calculated assuming coefficient of thermal expansion [24] of muscovite mica = $\alpha_d = 3.6 \times 10^{-5}\ ^\circ C^{-1}$.

TABLE VI Measured and calculated values of electrical resistivity of cast Al–4 wt % Cu–1.5 wt % Mg–mica particle composites

Alloy composition (wt %)	Volume fraction of matrix	Volume fraction of dispersed mica	Measured value of resistivity ($\times 10^{-6}\ \mu\Omega m$)	Electrical resistivity ($\mu\Omega m$) (theoretically calculated values)[*]		
				$\rho = \left[\dfrac{2 + V_d}{2 - 2V_d}\right]\rho_m$	$\rho = \dfrac{\rho_m \rho_d}{V_m \rho_d + V_d \rho_m}$	$\rho = \dfrac{\rho_m}{1 - 1.5 V_d}$
Al–4 Cu–1.5 Mg	1.00	0.00	3.59	3.590	3.59	3.59
Al–4 Cu–1.5 Mg–1.0 mica	0.99	0.01	3.81	3.626	3.626	3.644
Al–4 Cu–1.5 mica	0.985	0.015	3.89	3.644	3.645	3.672
Al–4 Cu–1.5 Mg–2 mica	0.98	0.02	4.29	3.663	3.663	3.701
Al–4 Cu–1.5 Mg–2.5 mica	0.975	0.025	4.81	3.681	3.682	3.729

[*]Calculated assuming the electrical resistivity [25] of muscovite mica = $\rho_d = 10^{21}\ \mu\Omega$.

friction conditions) increase the electrical resistivity only by 14%.

4. Conclusions

(1) Dispersions of increasing volumes of flake-shaped mica particles in the matrix of Al–4 wt % Cu–1.5 wt % Mg alloys progressively increases their damping capacity. At mica levels more than 2% the ratio of specific damping capacity to density of aluminium–mica composites is greater than that of flaky cast iron.

(2) The per cent increase in damping capacity of cast aluminium alloys due to a given volume of weakly-bonded fine mica powder is lower than the percentage reduction in damping capacity due to the same volume of coarser graphite suggesting that the type of particle has a greater effect on damping than the interfacial area.

(3) The average length of chips produced on machining aluminium–mica particle composites decreases progressively with volume of mica dispersions.

(4) The coefficient of thermal expansion of Al–4 wt % Cu–1.5 wt % Mg alloys increases very slightly with additions of up to 2.2% mica particles in the range 20 to 500° C. The measured increases are slightly higher compared to the values calculated using either the rule of mixtures or the Thomas formula.

(5) The electrical resistivity of aluminium alloy–mica composites increase with increasing amount of mica dispersed in the matrix. The measured increase in electrical resistivity as a result of 2% mica additions is 14% indicating that the composite is suitable for electrical contact applications.

References
1. F. A. BADIA and P. K. ROHATGI, *AFS Trans.* 2 (1969) 902.

2. *Idem, SAE Trans.* **76** (1969) 1200.
3. V. G. GORBUNDY, V. D. PARSHIN and V. V. PANIN, *Russ. Cast. Prod.* August (1974) 348.
4. B. C. PAI, P. K. ROHATGI and S. VENKATESH, *Wear* **30** (1974) 117.
5. B. C. PAI and P. K. ROHATGI, *Trans. Indian Inst. Met.* **27** (1974) 97.
6. P. K. ROHATGI and B. C. PAI, *Int. J. Lubric. Tech.* **101** (1979) 376.
7. A. M. PATTON, *J. Inst. Met.* **(C)** (1972) 197.
8. M. K. SURAPPA and P. K. ROHATGI, *Met. Tech.* **5** (1978) 358.
9. M. SUWA, K. MOMURO and K. SOONO, *Nippon Kinzoku, Grakkaishi* **41** (1977) 511.
10. B. C. PAI and P. K. ROHATGI, *J. Mater. Sci.* **13** (1978) 329.
11. S. RAY, B. C. PAI, K. V. PRABHAKAR and P. K. ROHATGI, *Mater. Sci. Eng.* **24** (1976) 31.
12. B. P. KRISHNAN, P. K. ROHATGI and H. R. SHETTY, *Trans. Amer. Foundrymens Soc.* **76–86** (1976) 73.
13. B. P. KRISHNAN, S. RAMAN and P. K. ROHATGI, Proceedings of the International Wear Conference, Michigan, USA, 1979, p. 160.
14. P. K. ROHATGI, B. C. PAI and P. C. PANDA, *J. Mater. Sci.* **14** (1979) 2277.
15. DEONATH, R. T. BHAT and P. K. ROHATGI, *J. Mater. Sci.* **15** (1980) 1241.
16. DEONATH, S. K. BISWAS and P. K. ROHATGI, *Wear* **60** (1980) 61.
17. P. K. ROHATGI, N. MURALI, H. R. SHETTY and R. CHANDRASEKHAR, *Mater. Sci. Eng.* **26** (1976) 115.
18. J. G. KAUFMAN, *Mater. Des. Eng.* (1962) 104.
19. M. A. O. FOX and R. D. ADAMS, *J. Mech. Eng. Sci.* **15** (1973) 81.
20. R. D. ADAMS and M. A. O. FOX, *J. Iron Steel Inst.* **211** (1977) 37.
21. E. P. BOWDEN and D. TABOR, "Friction and Lubrication Solids", (Clarendon Press, Oxford, 1974) p. 199.
22. V. K. AGRAWAL, Hindustan Aluminium Corporation, Renukoot, UP, India, private communication, July 1980.
23. P. S. TURNER, *J. Res. Natl. Bur. Std.* **37** (1946) 239.
24. J. P. THOMAS, "Effect of Inorganic Fillers on the Coefficient of Thermal Expansion of Polymeric Materials", General Dynamics/Fort Worth, Texas, AD 287–826. (As noted from *J. Composite Mater.* **1** (1967) 119.)
25. CHARLESS L. MANTELL, "Engineering Materials Handbook", (McGraw-Hill Book Co., New York, 1958) p. 35.
26. J. C. MAXWELL, A Treatise on Electricity and Magnetism", Vol. 1, 3rd edn, (Clarendon Press, Oxford, 1892) p. 440.
27. L. H. VAN VLACK, "Materials Science for Engineers", (Addison-Wesley Publishing Company, London, 1973) p. 407.
28. L. K. H. VAN BEEK, "Progress in Dielectrics", Vol. 7 (Heywood, London, 1967) p. 69.